Supramolecular Chemistry
Publication details, including instructions for authors and subscription information:
http://www.informaworld.com/smpp/title~content=t713649759

A new class of fluorescent chemosensors based on the β-aminobisphosphonate receptor

John F. Callan[a]; Sukanta Kamila[a]; Narinder Singh[a]; Ray C. Mulrooney[a]; Martha MacKay[a]; Maedhbh C. Cronin[a]; John Dunn[a]; David G. Durham[a]
[a] School of Pharmacy and Life Sciences, The Robert Gordon University, Aberdeen, UK

To cite this Article Callan, John F. , Kamila, Sukanta , Singh, Narinder , Mulrooney, Ray C. , MacKay, Martha , Cronin, Maedhbh C. , Dunn, John and Durham, David G.(2009) 'A new class of fluorescent chemosensors based on the β-aminobisphosphonate receptor', Supramolecular Chemistry, 21: 7, 643 — 649
To link to this Article: DOI: 10.1080/10610270802709352
URL: http://dx.doi.org/10.1080/10610270802709352

Supramolecular Chemistry
Vol. 21, No. 7, October–November 2009, 643–649

Taylor & Francis
Taylor & Francis Group

A new class of fluorescent chemosensors based on the β-aminobisphosphonate receptor

John F. Callan*, Sukanta Kamila, Narinder Singh, Ray C. Mulrooney, Martha MacKay, Maedhbh C. Cronin, John Dunn and David G. Durham

School of Pharmacy and Life Sciences, The Robert Gordon University, Aberdeen, UK

(*Received 8 August 2008; final version received 8 December 2008*)

The photophysical properties of a range of fluorescent sensors with β-aminobisphosphonate receptors have been studied. The compounds were designed according to the fluorophore–spacer–receptor format of photoinduced electron transfer-based sensors. The sensors displayed unusual fluorescence intensity–pH profiles that were attributed to a receptor–fluorophore H-bonding interaction that resulted in a quenching of fluorescence. The number of receptors and the nature of the fluorophore were both shown to have an effect on the pH profiles of the sensors. In addition, compound **1** was also shown to be selective for Cu^{2+} ions, in water at pH 7.4 with sensitivity in the micromolar range.

Keywords: fluorescence; sensor; pH; copper

1. Introduction

β-Aminobisphosphonate derivatives, such as pamidronate (Aredia), are commercially used to treat bone resorption disorders such as osteoporosis and Paget's disease (*1*). Their activity is thought to be due to the ability to strongly chelate certain metal ions, particularly Ca^{2+} (*2*). In addition, it has been demonstrated using electron paramagnetic spectroscopy that β-aminobisphosphonates derivatives bind strongly to Cu^{2+} (*3*). Therefore, their incorporation as the ionophore component of luminescent sensing assemblies seems a logical progression.

We have previously developed a luminescent sensor that incorporated β-aminobisphosphonate as a receptor component (*4*). The sensor, designed according to the fluorophore–spacer–receptor format of photoinduced electron transfer (PET)-based sensors (*5*), was shown to selectively bind Cu^{2+} ions in water at pH 7.4. However, the choice of naphthalene as fluorophore has obvious restrictions when considering intracellular applications, as UV excitation is necessary. Here, we improve on the design using anthracene as fluorophore by preparing {2-[anthracen-9-ylmethyl-(2-phosphono-ethyl)-amino]-ethyl}-phosphonic acid (**1**) and {2-[(10-{[bis-(2-phosphono-ethyl)-amino]-methyl}-anthracen-9-ylmethyl)-(2-phosphono-ethyl)-amino]-ethyl}-phosphonic acid (**3**). Both sensors were again constructed according to the PET design principle and differ only by the number of receptor ligands they possess. Control compounds were also prepared (**2** and **4**) in which the phosphonate receptors were absent. The preparation of these compounds has enabled us to propose a mechanism for the unusual pH profile of the sensors **1** and **3**. In particular, it has allowed us to correct upon a postulated mechanism for the pH behaviour of the aforementioned naphthalene-based compound from an earlier communication (*4*). The selectivity and sensitivity of **1** and **3** were also established against a range of common metal ions to determine their potential use as chemosensors.

2. Experimental

2.1 General

All reagents used were of the highest grade obtainable and were purchased from Aldrich. The compounds **5**, **7**–**8** and **10** were prepared with the literature methods (*4*, *13*, *15*). Absorbance measurements were recorded on an Agilent UV–vis spectrometer using 10-mm quartz cuvettes. Fluorescence measurements were recorded on a Shimadzu RF-5301 luminescence spectrometer using 10-mm quartz cuvettes. Excitation slit size was 10 nm and emission slit size was 10 nm. Scan speed was set at 500. The NMR spectra were recorded on a Bruker AVANCE 400 MHz spectrometer. Chemical shifts are reported in parts per million, downfield of TMS. Details of solvents are provided in Figures 1–6. Low-resolution MS was obtained on an Agilent 6130 Quadrupole LC/MS system. Accurate mass data were provided by the EPSRC National Mass Spectrometry Service, UK. Figure 3 was prepared on ArgusLab 4.0. The anthracene aminobisphosphonate was energy minimised and the binding site optimised by the rotation of the side chains.

*Corresponding author. Email: j.callan@rgu.ac.uk

ISSN 1061-0278 print/ISSN 1029-0478 online

DOI: 10.1080/10610270802709352
http://www.informaworld.com

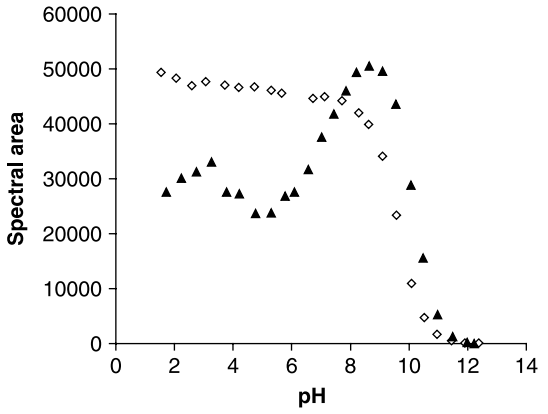

Figure 1. Plot of fluorescent intensity against pH for **1** (▲) and **2** (◇). [**1**] = 4.40 × 10^{-6} M and [**2**] = 1.88 × 10^{-6} M, λ_{ex} = 370 nm.

2.2 Synthesis of (2-{anthracen-9-ylmethyl-[2-(diethoxy-phosphoryl)-ethyl]-amino}-ethyl)-phosphonic acid diethyl ester (6)

A mixture of 9-(aminomethyl)anthracene (0.97 g, 4.72 mmol) and diethyl vinylphosphonate (4.42 ml, 28.3 mmol) was heated at reflux in dry methanol (20 ml) for 10 days. Following cooling of the reaction mixture, the solvent was removed under reduced pressure. The crude product was purified by flash chromatography using silica gel eluted with methanol:dichloromethane (1:50). The product was separated as an orange liquid (0.29 g, 11%); δ_H (400 MHz, DMS0-d_6) 1.08 (12H, t, J = 6.4 Hz, —OCH$_2$CH_3), 1.95 (4H, m, —CH$_2$CH_2P(O)(OEt$_2$)$_2$), 2.81 (4H, m, —NCH_2CH$_2$—), 3.85 (8H, m, —OCH_2CH$_3$), 4.59 (2H, s, —CH_2N—), 7.56 (4H, m, Ar-H), 8.09 (2H, d, J = 8.0 Hz, Ar-H) and 8.55 (3H, m, Ar-H); δ_C (100 MHz, DMS0-d_6) 16.0, 21.4, 22.76, 45.7, 49.2, 123.4, 123.9, 125.0, 127.1, 129.2, 130.3, 130.9 and 134.5; *m/z* (ES-MS) 536 (60%) [M^+], 400 (100%) and 191 (24%); HR-MS calcd for $C_{27}H_{39}NO_6P_2$, 536.2325; found, 536.2322.

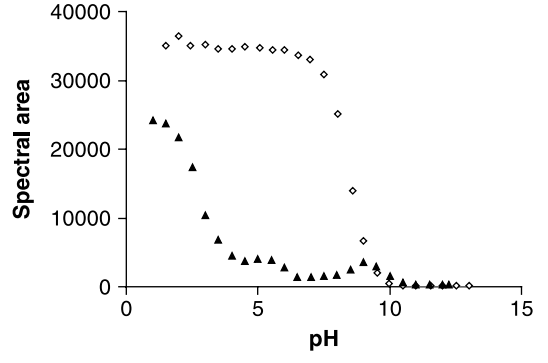

Figure 2. Plot of fluorescent intensity against pH for **3** (▲) and **4** (◇). [**3**] = 2.25 × 10^{-6} M and [**4**] = 2.87 × 10^{-6} M, λ_{ex} = 370 nm.

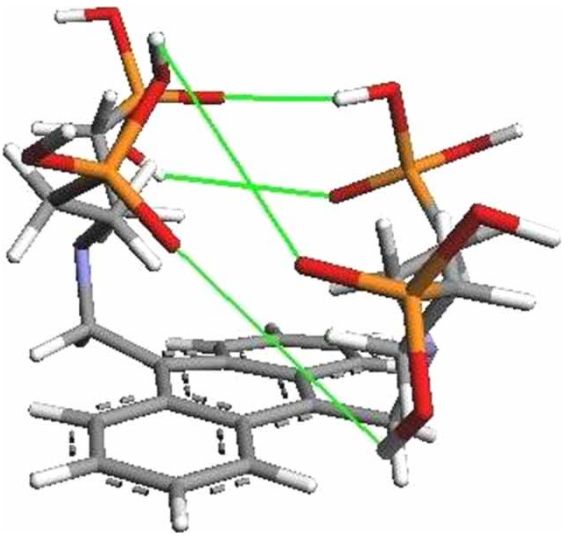

Figure 3. Illustration of potential intramolecular H-bonding between phosphonate groups on one side of **3** at low pH.

2.3 Synthesis of {2-[anthracen-9-ylmethyl-(2-phosphono-ethyl)-amino]-ethyl}-phosphonic acid (1)

To a solution of **6** (0.12 g, 0.23 mmol) in dry CH_2Cl_2 (10 ml) was added bromotrimethylsilane (0.82 ml, 6.31 mmol). The mixture was stirred overnight at room temperature. Evaporation of the solvent along with excess bromotrimethylsilane under reduced pressure afforded the crude product, which was triturated with hexane. The resulting solid was dissolved in DCM and the product was obtained after precipitation with ether (0.092 g, 98%); mp 172°C; δ_H (400 MHz, MeOD) 2.1 (4H, m, —CH$_2$CH_2-P(O)(OH)$_2$), 3.6 (4H, m, —NCH_2CH$_2$—), 5.5 (2H, s, —CH_2N—), 7.65 (4H, m, Ar-H), 8.2 (2H, d, J = 8.0 Hz, Ar-H), 8.45 (2H, d, J = 8 Hz, Ar-H) and 8.85 (1H, s, Ar-H); δ_C (100 MHz, MeOD) 22.7, 24.2, 51.8, 120.7, 124.0, 126.8, 129.4, 129.6, 130.9, 132.8 and 133.0; *m/z* (ES-MS) 423

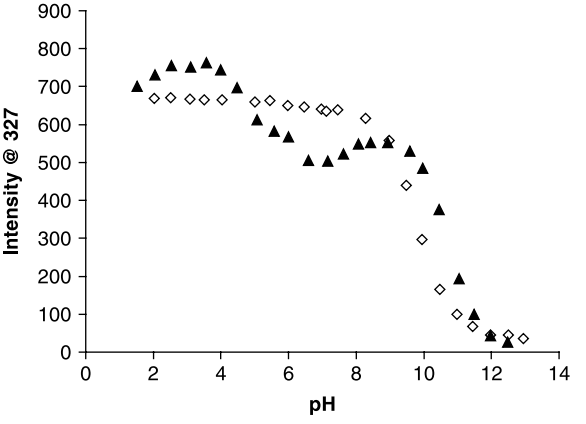

Figure 4. Plot of fluorescent intensity against pH for **10** (▲) and **11** (◇). [**10**] = 8.57 × 10^{-7} M and [**11**] = 3.8 × 10^{-7} M, λ_{ex} = 283 nm.

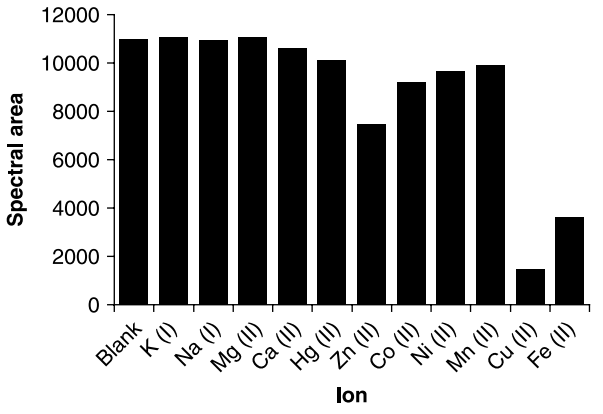

Figure 5. Selectivity data for sensor **1** against a range of common metal ions as their chloride salts in 0.01 M HEPES buffer at pH 7.4. [**1**] = 1.6×10^{-7} M, [metal ion] = 1×10^{-4} M, $\lambda_{ex} = 370$ nm.

(25%) [M^+], 232 (50%) and 121 (100%); HR-MS calcd for $C_{19}H_{23}NO_6P_2$ $(M-H)^-$, 422.0928; found, 422.0923.

2.4 Synthesis of anthracen-9-ylmethyl-diethylamine (2)

A mixture of 9-(chloromethyl)anthracene (1.080 g, 4.41 mmol), diethylamine (1.37 ml, 13.23 mmol) and DIPEA (2.3 ml, 13.23 mmol) in anhydrous 1,4-dioxane (10 ml) was stirred at 100°C overnight. The solution was allowed to cool, and excess solvent and unreacted amine were removed by evaporation under reduced pressure. The crude product was then washed with distilled water and extracted with ethyl acetate. The organic layer was dried over Na_2SO_4 and the solvent removed under reduced pressure to afford the product (0.89 g, 82.54%); mp 84°C; δ_H (400 MHz, $CDCl_3$) 1.00 (6H, t, $J = 6.5$ Hz, —NCH_2CH_3), 2.55 (4H, q, $J = 7.0$ Hz, —NCH_2CH_3), 4.45 (2H, s, —$CH_2NCH_2CH_3$), 7.45 (4H, m, Ar-H), 7.9 (2H, d, $J = 8.5$ Hz, Ar-H), 8.30 (1H, s, Ar-H) and 8.50 (2H, d, $J = 8.0$ Hz, Ar-H); δ_C (100 MHz, $CDCl_3$) 10.9, 45.6, 49.2, 122.8, 123.9, 124.6, 126.4, 127.9, 130.4, 132.4 and 132.9; *m/z* (ES-MS) 264 (10%) (M^+) and 191 (100%); HR-MS calcd for $C_{19}H_{21}N$, 264.1747; found, 264.1750.

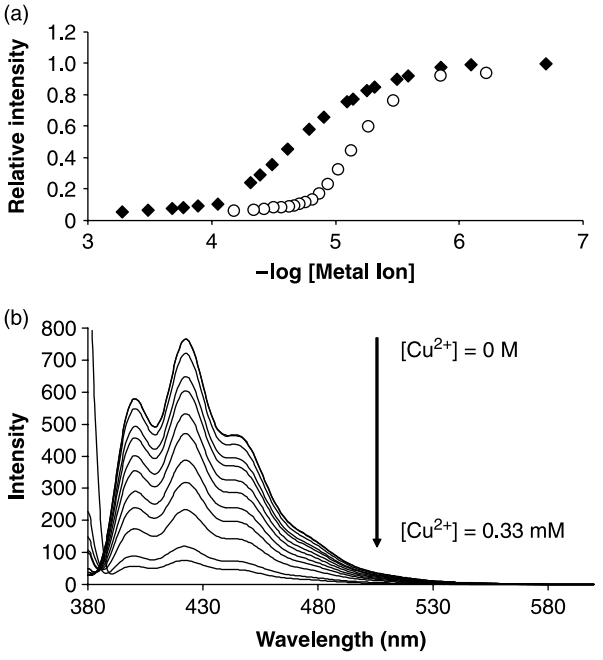

Figure 6. (a) Plot of relative intensity of **1** against − log [metal ion] for Cu (II) (◆) and Fe (II) (○) as their chloride salts in 0.01 M HEPES buffer at pH 7.4. (b) Effect of the Cu^{2+} ion concentration on the fluorescent intensity of **1**. [**1**] = 1.6×10^{-7} M, $\lambda_{ex} = 370$ nm.

2.5 Synthesis of (2-{[10-({bis-[2-(diethoxy-phosphoryl)-ethyl]-amino}-methyl)-anthracen-9-ylmethyl]-[2-(diethoxy-phosphoryl)-ethyl]-amino}-ethyl)-phosphonic acid diethyl ester (9)

The procedure for the preparation of **6** was followed using the following amounts of reagents: **8** (1 g, 4.23 mmol) and diethylvinyl phosphonate (8.58 ml, 55.0 mmol). The product was obtained as an orange solid (0.54 g, 16.7%); mp 115°C; δ_H (400 MHz, MeOD) 1.05 (24H, m, 8 × –CH_3), 1.87 (8H, m, 4 × —CH_2P—), 2.76 (8H, m, 4 × –NCH_2—), 3.70 (16H, m, 8 × —OCH_2—), 4.51 (4H, s, 2 × Ar—CH_2), 7.42 (4H, dd, $J_1 = 3.5$ Hz, $J_2 = 8.0$ Hz, Ar-H), 8.47 (4H, dd, $J_1 = 3.5$ Hz, $J_2 = 3.0$ Hz, Ar-H); δ_C (100 MHz, MeOD) 16.6, 22.9, 24.3, 46.8, 51.2, 126.6, 127.9, 131.6 and 132.4; *m/z* (ES-MS) 894 (5%) [M^+], 548 (10%), 447 (100%) [M^{2+}] and 346 (15%); HR-MS calcd for $C_{40}H_{68}N_2O_{12}P_4$, 893.3795; found, 893.3810.

2.6 Synthesis of {2-[(10-{[bis-(2-phosphono-ethyl)-amino]-methyl}-anthracen-9-ylmethyl)-(2-phosphono-ethyl)-amino]-ethyl}-phosphonic acid (3)

The procedure for the preparation of **1** was followed using the following amounts of reagents: **9** (0.54 g, 0.60 mmol) and bromotrimethylsilane (1.26 ml, 9.60 mmol). The product was obtained as an orange solid (0.12 g, 30%). δ_H (400 MHz, MeOD) 2.00 (8H, m, 4 × —CH_2P—), 3.30 (8H, t, 4 × —NCH_2—), 5.67 (4H, s, 2 × Ar—CH_2), 7.77 (4H, dd, $J_1 = 3.0$ Hz, $J_2 = 7.5$ Hz, Ar-H) and 8.48 (4H, dd, $J_1 = 3.0$ Hz, $J_2 = 7.5$ Hz, Ar-H); δ_C (100 MHz, MeOD) 20.8, 22.2, 48.1, 123.6, 123.8, 127.7 and 130.5; *m/z* (ES-MS) 668 (20%) [M^+], 588 (60%), 560 (60%) and 349 (100%); HR-MS calcd for $C_{24}H_{36}N_2O_{12}P_4$ $(M-H)^-$, 667.1146; found, 667.1139.

2.7 Synthesis of (10-diethylaminomethyl-anthracen-9-ylmethyl)-diethylamine (4)

The procedure for the preparation of **2** was followed using the following amounts of reagents: **7** (1.00 g, 2.75 mmol),

diethylamine (1.72 ml, 16.54 mmol) and *N*-ethyldiisopropylamine (2.88 ml, 16.54 mmol). The product was obtained as an orange solid (0.72 g, 75.2%); mp 227°C; δ_H (400 MHz, DMSO) 1.23 (12H, t, 4 × —C*H*$_3$), 3.05 (4H, m, 2 × —NC*H*$_2$—), 3.29 (4H, m, 2 × —NC*H*$_2$—), 5.47 (4H, s, 2 × Ar—C*H*$_2$), 7.77 (4H, m, Ar-H) and 8.54 (4H, m, Ar-H); δ_C (100 MHz, DMSO) 8.7, 47.2, 48.4, 125.3, 125.5, 127.4 and 130.9; *m/z* (ES-MS): 276 (100%), 204 (6%) and 175 (11%) [M^{2+}]. HR-MS calcd for $C_{24}H_{32}N_2$, 349.2638; found, 349.2634.

2.8 Synthesis of diethyl-naphthalen-1-ylmethylamine (11)

The procedure for the preparation of **2** was followed using the following amounts of reagents: 1-(chloromethyl)-naphthalene (2.22 ml, 14.15 mmol), diethylamine (4.40 ml, 42.45 mmol) and *N*-ethyldiisopropylamine (7.39 ml, 42.46 mmol). The product was obtained as dark viscous liquid (2.61 g, 84.2%); δ_H (400 MHz, $CDCl_3$) 0.99 (6H, t, $J = 6.2$ Hz, 2×—C*H*$_3$), 2.49 (4H, m, 2×—NC*H*$_2$—), 3.90 (2H, s, Ar—C*H*$_2$—), 7.31 (4H, m, Ar-H), 7.50 (1H, d, $J = 7.5$ Hz, Ar-H), 7.66 (1H, d, $J = 7.5$ Hz, Ar-H) and 7.72 (1H, d, $J = 7.5$ Hz, Ar-H); δ_C (100 MHz, $CDCl_3$) 11.8, 47.0, 56.3, 124.8, 125.6, 125.9, 127.4, 127.6, 127.8, 128.6, 132.7, 134.0 and 135.9; *m/z* (ESMS) 214 (100%) [M^+] and 141 (25%); HRMS calcd for $C_{15}H_{19}N$, 214.1590; found, 214.1591.

3. Results and discussion

3.1 Synthesis of sensors (1 and 3) and control compounds (2 and 4)

The synthesis of the target and control compounds is shown in Scheme 1. Compound **1** was formed by first converting 9-chloromethylanthracene to 9-aminomethyl anthracene (**5**) using the Delepine reaction (*6*). Following the Michael addition of **5** with diethylvinyl phosphonate and subsequent hydrolysis with bromotrimethylsilane, sensor **1** was isolated as a white solid. Control compound **2** was also formed from chloromethyl anthracene by direct reaction with diethylamine.

A similar strategy was followed for the preparation of compound **3**. Bisbromomethyl anthracene (**7**) was obtained from anthracene after reaction with hydrobromic acid. This was then converted to **3** following similar chemistry as outlined above. The control compound **4** was also formed from 9,10-bisbromomethyl anthracene by reaction with diethylamine.

3.2 pH titration of 1 and 2

The UV analysis of both compounds showed characteristic anthracene absorbance with a λ_{MAX} centred at ~370 nm. The emission spectra, when excited at 370 nm, were also characteristic of anthracene-based compounds, with three distinct bands observed at 401, 422 and 444 nm. However, the dependence of their emission on solution pH was markedly different. A plot of fluorescent intensity against pH is shown in Figure 1. The sigmoidal profile of control compound **2** ($\Phi = 0.16$) was typical of a PET sensor with a tertiary amine as the receptor, with fluorescence switching 'on' over two log units (*7*). The emission intensity was low at high pH due to PET from the tertiary amine to the anthracene fluorophore. As pH was lowered, the tertiary amine became protonated, its oxidation potential raised and PET cancelled, allowing fluorescence to 'switch on' (*8*). Using a plot of $-\log (F_{MAX} - F)/(F - F_{MIN})$ against pH (where F_{MAX} is the maximum fluorescence intensity, F_{MIN} the minimum fluorescence intensity and F the measured fluorescence intensity), the pK_a of the tertiary amine was calculated as 9.43 (*9*; Table 1).

The pH titration of sensor **1** ($\Phi = 0.22$) also switches 'on' fully at pH 9 (p$K_a = 10.24$), but then, the intensity falls off between pH 8 and 5. This initial switching 'on' can again be attributed to the protonation of the tertiary amine cancelling PET as in the case of the control, the pK_a value being consistent with that found for the amino group in alkyl aminobisphosphonates determined by potentiometric titration (*3*).

The reduction in fluorescence intensity between pH 8 and 5 can be explained by the protonation of the phosphonate oxyanions and their hydrogen bonding with the π-electron cloud of the anthracene. The intramolecular quenching of anthracene emission by carboxylic acid groups has been demonstrated earlier (*7*, *10*). The flexibility of the receptor unit in **1** means that the approach of the phosphonic acid group with the anthracene π-cloud is also feasible for **1**. The slight rise and then fall in fluorescence intensity between pH 5 and 2 is probably due to the stepwise protonation of the phosphonate groups before they interact with the anthracene π-system.

3.3 pH titration of 3 and 4

Figure 2 shows a plot of fluorescence intensity against pH for compounds **3** and **4**. The control compound shows a typical sigmoidal profile with fluorescence switching 'on' over two log units. Both tertiary amines must be protonated before fluorescence switches 'on' as there are two PET channels present in the molecule. The calculated pK_a of 8.34 of **4** ($\Phi = 0.12$) is approximately one log unit lower than in **2**. Again, the profile of sensor **3** ($\Phi = 0.09$) is markedly different from that of the control. The fluorescence remains low until approximately pH 4 when it switches 'on' dramatically. There is also evidence of a small rise in intensity from ~ pH 12 to 9 (pK_a 8.34), which

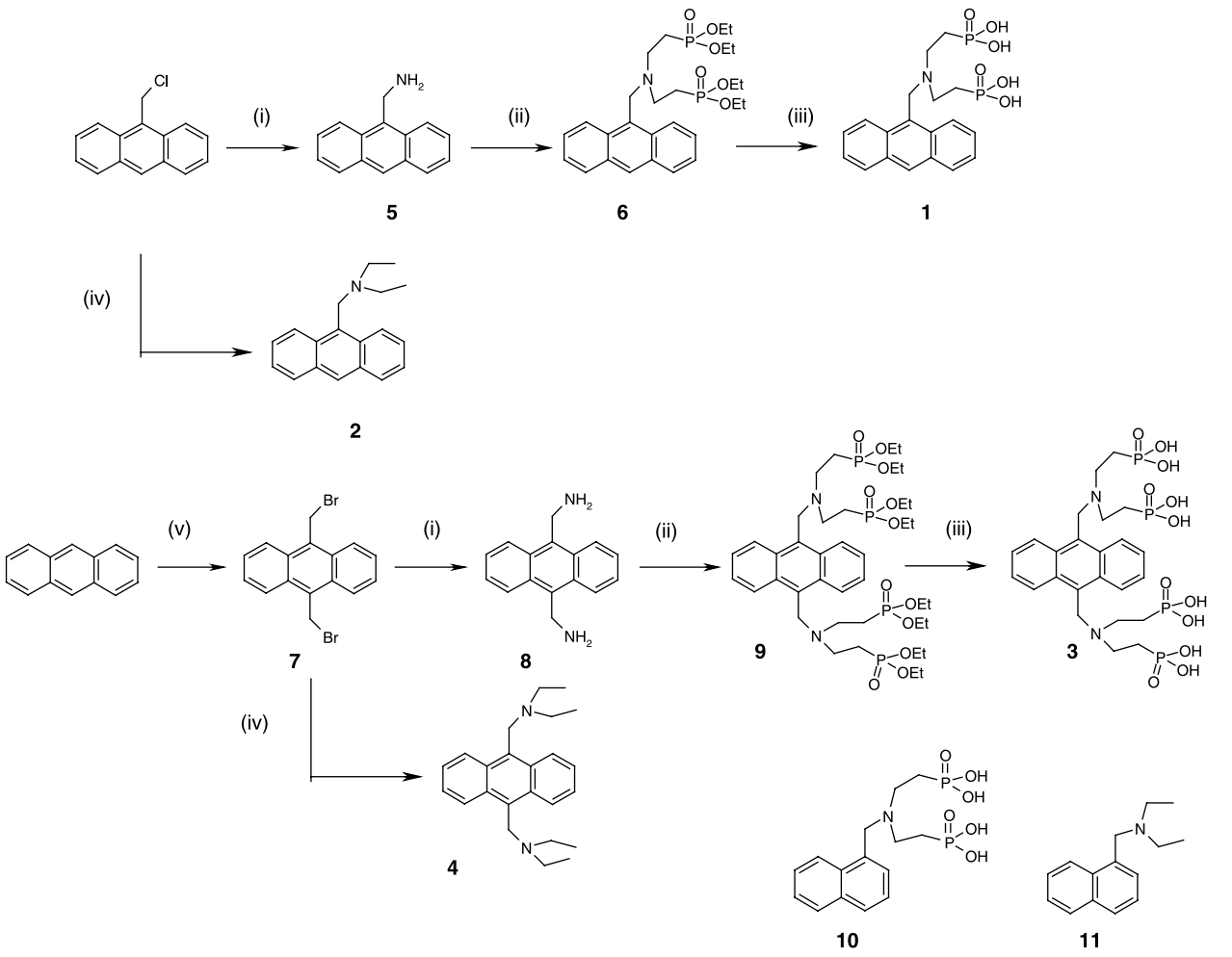

Scheme 1. Synthesis of compounds **1**–**4**. (i) $C_6H_{12}N_4$, dry $CHCl_3$, 80°C, 5 h; (ii) $CH_2CHPO(OCH_2CH_3)_2$, dry MeOH, 80°C, 10 days; (iii) $(CH_3)_3SiBr$, dry CH_2Cl_2, 28°C, 18 h; (iv) $(CH_3CH_2)_2NH$, DIPEA, dry $C_4H_8O_2$, 100°C, 18 h and (v) HBr, CH_3COOH, $CH_3(CH_2)_{13}N(Br)(CH_3)_3$, $C_3H_6O_3$, 100°C, 18 h.

falls off between pH 9 and 7. This can again be explained as in the case of **1**, with the rise due to the protonation of the tertiary amine, and the fall off due to oxyanion protonation and subsequent hydrogen bonding with the anthracene π-cloud. The much more effective quenching of fluorescence for **3** compared with **1** is most likely due to a stronger interaction between the protonated oxyanions and the anthracene π-cloud, due to the presence of the second receptor ligand. A second small step is also evident between pH 7 and 5 ($pK_a = 5.99$), which, again, may be explained by a stepwise protonation of the phosphonate groups before interaction with the anthracene π-cloud.

Table 1. Photophysical properties of **1**–**4** and **11**.

Property	$\lambda_{MAX\,ABS}$	$\lambda_{MAX\,EM}$	ε_{MAX} ($mol^{-1}\,dm^3\,cm^{-1}$)	pK_a (amino)	pK_a (phosphate)	Φ_{FLU}[a]	Log β
1	369	422	7485	10.24	–	0.22	–
2	368	421	9259	9.43	–	0.16	–
3	367	426	6601	8.34	2.80, 5.99	0.09	–
4	368	428	8212	8.34	–	0.12	–
11	283	333	5610	9.91	–	0.08	–
1 + Cu(II)	–	422	–	–	–	–	4.72
1 + Fe(II)	–	421	–	–	–	–	5.23

[a] Quantum yields (Φ) for **1**–**4** were calculated with reference, to anthracene, while **11** was calculated with reference to tryptophan (*11*). Φ for **1** and **3** was recorded in H_2O at pH 7.4, while **2** and **4** were recorded in EtOH.

But what causes the large enhancement in fluorescence on going from pH 4 to 2? The hydrogen bonding effect of the phosphonate groups with the anthracene π-cloud must be turned off in some manner.

We believe this can be best explained as follows: the full protonation of the phosphonate groups, coupled with the flexibility of the receptor units, enables a strong hydrogen-bonding interaction of the phosphonate groups with each other. That is, the phosphonate groups on one side of the anthracene molecule (the 9-position) interact strongly with those on the opposite side of the molecule (the 10-position) by bending to one side of the π-system, as depicted in Figure 3. This strong hydrogen bonding interaction is at the expense of the hydrogen bonding with the anthracene π-cloud and enables fluorescence to switch 'on'. However, as observed in Figure 2, the intensity maxima of the sensor are somewhat smaller than in the control, indicating that a residual phosphonate–anthracene π-cloud quenching interaction still exists, even at pH 1.0.

The mechanistic interpretation outlined above for the unusual pH profile of compounds **1** and **3** is different from that previously postulated by us in an earlier communication. For purposes of clarity, we include the fluorescent intensity–pH profile for {2-[naphthalen-1-ylmethyl-(2-phosphono-ethyl)amino]ethyl}-phosphonic acid (**10**) used in that study along with its control analogue (**11**) in Figure 4. The profile of **10** is similar to **1** in that it switches 'on' at high pH, switches 'off' slightly at intermediate pH and then back 'on' at low pH. However, the magnitude of the decrease in intensity at intermediate pH is much smaller for **10** than for **1**. In addition, the intensity of **10** at low pH (i.e. pH 2) is about that of its control **11** (i.e. it is fully switched 'on'), while the intensity of **1** at the same pH is about half that of the control. We previously accounted for the intensity increase of **10** from pH 12 to 10 as being due to intramolecular proton transfer from a protonated phosphonate group to the tertiary amine of the receptor, resulting in a partial cancellation of the PET process. The second stepped increase in intensity from pH 6 to 4 was attributed due to full protonation of the tertiary amine and a complete cancellation of the PET process. We now consider this to be an inaccurate description for the profile of **10** and believe that the same reasons as offered for **1** and **3** are also evident for **10**. That the reduction in intensity between pH 9 and 7 is much less dramatic for **10** than **1** is most likely due to the much smaller π-cloud of naphthalene compared with anthracene, leading to a reduced effectiveness of the phosphonate–π-cloud hydrogen bonding interaction and a reduced quench.

3.4 Selectivity and sensitivity measurements of 1 and 3

The nature of the pH–fluorescence profile of **1** means that its use as an off–on sensor for physiologically relevant analytes is limited, as its fluorescence remains 'on' over a wide pH range. However, as the fluorescence intensity is quite high at pH 7.4, **1** may be effective as an 'on–off' sensor in buffered solution. We screened **1** against a range of common metal ions, in 0.01 M HEPES buffer at pH 7.4. As shown in Figure 5, addition of Cu^{2+} leads to an ~80% quenching of the original fluorescent intensity, while Fe^{2+} and Zn^{2+} led to quenches of ~60 and ~20%, respectively, with the other ions having virtually no effect. The quenching effect of Cu^{2+} is expected as the open-shell ion is known to quench fluorescence by electron and/or energy transfer (*5e*). Also, its position in the Irving Williams series means it is a strong binder to ligands, irrespective of the nature or number of ligands involved (*11*). The quenching effect from Fe^{2+} is most likely due to an inner filter effect (*12*), but the quenching effect from the closed-shell Zn^{2+}, although minor, was not expected. By contrast, the addition of these ions to a solution of the control produced negligible quenching, highlighting the requirement of the aminobisphosphonate receptor for analyte binding. Figure 6 shows a plot of relative intensity against $-\log$ [anion] for Cu^{2+} and Fe^{2+}. Both ions quench fluorescence over two log units, indicating a 1:1 binding between sensor and metal ions (*13*). The binding constants, $\log \beta$, calculated from Equation (1) were 4.72 and 5.23 for Cu^{2+} and Fe^{2+}, respectively (*9*).

$$-\log(F_{MAX} - F)/(F - F_{MIN}) = \log\,[\text{anion}] + \log \beta \quad (1)$$

This confirms that Fe^{2+} binds stronger to the sensor than Cu^{2+} as observed for **10** in a previous study (*4*). The sensitivity of **1** for Cu^{2+} is in the physiologically relevant range (*14*), and the quenching effect caused by Fe^{2+} can be cancelled by the addition of fluoride ion to produce the colourless FeF_6^{3-} (*12*). Therefore, **1** could be utilised as a water-soluble sensor for Cu^{2+}, operable in the physiological range. The low fluorescence intensity of **3** at pH 7.4 means it is potentially suitable as an 'off–on' sensor, provided analyte binding is sufficient to disrupt the intramolecular hydrogen bonds between the phosphonate groups and the anthracene π-cloud. Unfortunately, when tested against the same metal ions listed in Figure 4, no fluorescence enhancements were observed, suggesting that the phosphonate–anthracene π-cloud interaction must be relatively strong.

4. Conclusion

We have presented a new class of fluorescent sensors whose response to pH varies considerably depending on both the number of receptors attached and the nature of the fluorophore. The reason for the unusual pH profile for these compounds has been attributed to a phosphonate–fluorophore π-cloud hydrogen bonding interaction that quenches fluorescence. To the best of our knowledge, this

is the first reported example of such an effect with phosphonates on anthracene. In the case of compound **3**, this attraction can be broken at very low pHs when all the phosphonate oxyanions are protonated. In addition, compound **1** showed good selectivity for Cu^{2+} ions in water at pH 7.4 and its sensitivity was determined to be in the physiological range.

Acknowledgements

The authors would like to thank RGU and the Leverhulme Trust, UK for financial support and Professor A.P. de Silva and Dr Bridgeen McCaughan for their helpful discussions. We also thank the EPSRC National Mass Spectrometry Service for the high-resolution spectra.

References

(1) British National Formulary, Royal Pharmaceutical Society of Great Britain, 2005; Vol. 49, 383 pp.

(2) (a) Kiss, T.; Balla, J.; Nagy, G.; Kozlowski, H.; Kowalik, J. *Inorg. Chim. Acta* **1987**, *138*, 25–30. (b) Kiss, T.; Farkas, E.; Kozlowski, H. *Inorg. Chim. Acta* **1989**, *155*, 281–287. (c) Matczak-Jon, E.; Kurzak, B.; Sawka-Dobrowolska, W.; Kafarski, P.; Lejczak, B. *J. Chem. Soc. Dalton Trans*. **1996**, *16*, 3455–3464. (d) Matczak-Jon, E.; Kurzak, B.; Sawka-Dobrowolska, W.; Lejczak, B.; Kafarski, P. *J. Chem. Soc. Dalton Trans*. **1998**, *1*, 161–170. (e) Gumienna-Kontecka, E.; Jezierska, J.; Lecouvey, M.; Leroux, Y.; Kozlowski, H. *J. Inorg. Biochem.* **2002**, *89*, 13–17. (f) Kubicek, V.; Vojtísek, P.; Rudovsky, J.; Hermann, P.; Lukes, I. *Dalton Trans*. **2003**, *20*, 3927–3938.

(3) Gumienna-Kontecka, E.; Galezowska, J.; Drag, M.; Latajka, R.; Kafarski, P.; Kozlowski, H. *Inorg. Chim. Acta* **2004**, *357*, 1632–1636.

(4) Kamila, S.; Callan, J.F.; Mulrooney, R.C.; Middleton, M. *Tetrahedron Lett.* **2007**, *48*, 7756–7760.

(5) (a) Tsien, R.Y. *Am. J. Physiol.* **1992**, *26*, C723–C728. (b) Bissell, R.A.; de Silva, A.P.; Gunaratne, H.Q.N.; Lynch, P.L.M.; Maguire, G.E.M.; McCoy, C.P.; Sandanayake, K.R.A.S. *Top. Curr. Chem.* **1993**, *168*, 223–264. (c) Czarnik, A.W. *Adv. Supramol. Chem.* **1993**, *3*, 131–157. (d) Czarnik, A.W. *Acc. Chem. Res.* **1994**, *27*, 302–308. (e) Fabbrizzi, L.; Poggi, A. *Chem. Soc. Rev.* **1995**, *24*, 197–202. (f) de Silva, A.P.; Gunaratne, H.Q.N.; Gunnlaugsson, T.; Huxley, A.J.M.; McCoy, C.P.; Rademacher, J.T.; Rice, T.E. *Chem. Rev.* **1997**, *97*, 1515–1566. (g) Fabbrizzi, L.; Licchelli, M.; Pallavicini, P. *Acc. Chem. Res.* **1999**, *32*, 846–853. (h) Fabbrizzi, L. *Coord. Chem. Rev.* **2000**, *205*, 1–2. (i) Kojima, H.; Nagano, T. *Adv. Mater.* **2000**, *12*, 763–765. (j) Rurack, K.; Resch-Genger, U. *Chem. Soc. Rev.* **2002**, *31*, 116–127. (k) de Silvia, A.P.; McClean, G.D.; Moody, T.S.; Weir, S.M. In *Handbook of Photochemistry and Photobiology*; Nalwa, H.S., Ed.; American Scientific Publishers: Stevenson Ranch, CA, 2003. (l) Martínez-Máñez, R.; Sancenón, F. *Chem. Rev.* **2003**, *103*, 4419–4476. (m) Callan, J.F.; de Silvia, A.P.; Magri, D.C. *Tetrahedron* **2005**, *61*, 8551–8588.

(6) Surrey, A.R. *Named Reactions in Organic Synthesis*; Academic Press Inc.: New York, NY and London, 1961.

(7) Callan, J.F.; de Silva, A.P.; McClenaghan, N.D. *Chem. Commun.* **2004**, *18*, 2048–2049.

(8) Magri, D.C.; Callan, J.F.; de Silva, A.P.; Fox, D.P.; McClenaghan, N.D.; Sandanayake, K.R.A.S. *J. Fluoresc.* **2005**, *15*, 769–775.

(9) (a) de Silva, A.P.; Gunaratne, H.Q.N. *J. Chem. Soc. Chem. Commun.* **1990**, 186–188. (b) de Silva, A.P.; Gunaratne, H.Q.N.; Lynch, P.L.M. *J. Chem. Soc. Perkin Trans*. **1995**, *2*, 685–690.

(10) Eaton, D.F. *Pure Appl. Chem.* **1988**, *60*, 1107–1114.

(11) Rurack, K. *Spectrochim. Acta A* **2001**, *57*, 2161–2195.

(12) Xie, H.Y.; Liang, J.G.; Zhang, Z.L.; Liu, Y.; He, Z.K.; Pang, D.W. *Spectrochim. Acta A* **2004**, *60*, 2527–2530.

(13) Gunnlaugsson, T.; Davis, A.P.; Hussey, G.M.; Tierney, J.; Glynn, M. *Org. Biomol. Chem.* **2004**, *2*, 1856–1863.

(14) Gunnlaugsson, T.; Leonard, J.P.; Sénéchal, K.; Harte, A.J. *Chem. Commun.* **2004**, 782–783.

(15) Gunnlaugsson, T.; Davis, A.P.; O'Brien, J.E.; Glynn, M. *Org. Biomol. Chem.* **2005**, *3*, 48–56.